ADVANCED BIOLOGY

Supporting Information

for *Adv. Biology,* DOI: 10.1002/adbi.202101017

High-Yield Production, Characterization, and Functionalization of Recombinant Magnetosomes in the Synthetic Bacterium *Rhodospirillum rubrum "magneticum"*

*Frank Mickoleit, Sabine Rosenfeldt, Mauricio Toro-Nahuelpan, Miroslava Schaffer, Anna S. Schenk, Jürgen M. Plitzko, and Dirk Schüler**

Supporting Information

High-Yield Production, Characterization and Functionalization of Recombinant Magnetosomes in the Synthetic Bacterium *Rhodospirillum rubrum "magneticum"*

*Frank Mickoleit, Sabine Rosenfeldt, Mauricio Toro-Nahuelpan, Miroslava Schaffer, Anna S. Schenk, Jürgen M. Plitzko, and Dirk Schüler**

Dr. F. Mickoleit, Prof. Dr. D. Schüler
Dept. Microbiology, University of Bayreuth, D-95447 Bayreuth, Germany
E-mail: dirk.schueler@uni-bayreuth.de

Dr. S. Rosenfeldt
Bavarian Polymer Institute (BPI) / Physical Chemistry 1, University of Bayreuth, D-95447 Bayreuth, Germany

Dr. M. Toro-Nahuelpan
Dept. Microbiology, University of Bayreuth, D-95447 Bayreuth, Germany
Dept. Molecular Structural Biology, Max Planck Institute of Biochemistry, D-82152 Martinsried, Germany
Present address: EMBL Heidelberg, Structural and Computational Biology Unit, D-69117 Heidelberg, Germany

Dr. M. Schaffer, Prof. Dr. J. M. Plitzko
Dept. Molecular Structural Biology, Max Planck Institute of Biochemistry, D-82152 Martinsried, Germany

Jun.-Prof. Dr. A. S. Schenk
Bavarian Polymer Institute (BPI) / Physical Chemistry - Colloidal Systems, University of Bayreuth, D-95447 Bayreuth, Germany

Supplemental Figures

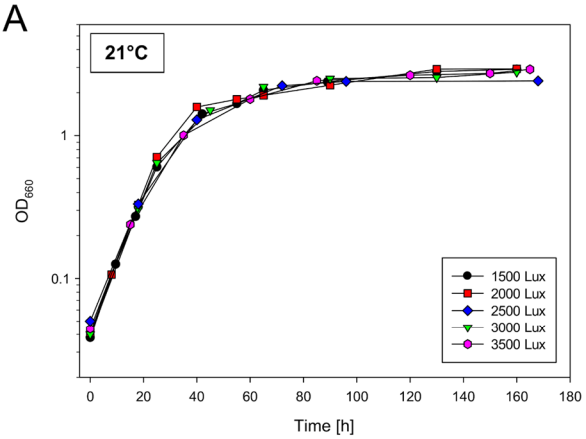

Light intensity [lux]	OD_{660}	Generation time [h]	C_{mag}	Fe content [% dry weight]
1500	2.24 ± 0.21	6.9 ± 0.5	0.37 ± 0.03	0.13
2000	2.36 ± 0.14	6.9 ± 0.4	0.34 ± 0.04	0.12
2500	2.42 ± 0.22	6.8 ± 0.5	0.34 ± 0.04	0.12
3000	2.24 ± 0.18	6.7 ± 0.7	0.35 ± 0.05	0.11
3500	2.48 ± 0.19	6.7 ± 0.5	0.27 ± 0.07	0.10

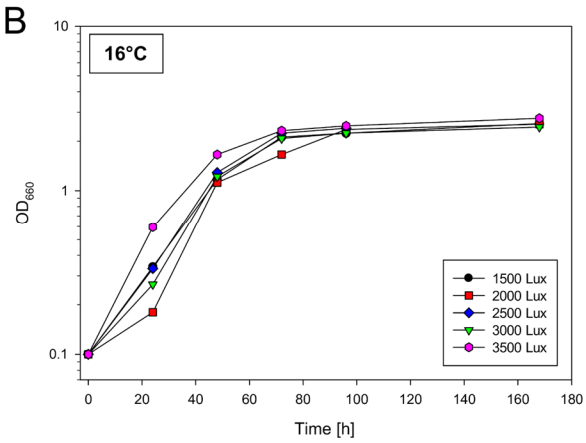

Light intensity [lux]	OD_{660}	Generation time [h]	C_{mag}	Fe content [% dry weight]
1500	2.56 ± 0.30	13.5 ± 2.1	0.37 ± 0.05	0.11
2000	2.54 ± 0.23	13.8 ± 1.8	0.36 ± 0.04	0.14
2500	2.42 ± 0.31	13.0 ± 2.0	0.34 ± 0.06	0.13
3000	2.44 ± 0.24	13.3 ± 1.4	0.33 ± 0.05	0.14
3500	2.76 ± 0.51	13.6 ± 1.3	0.29 ± 0.06	0.10

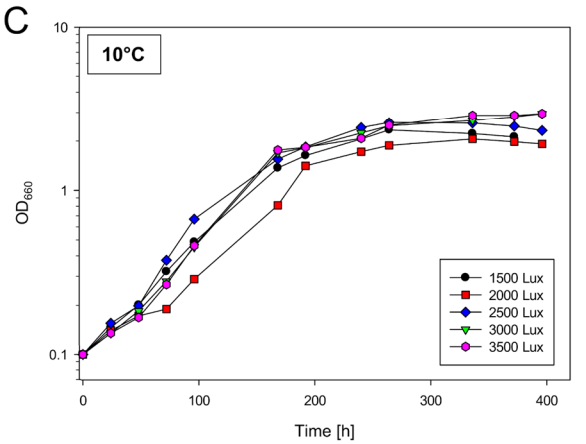

Light intensity [lux]	OD_{660}	Generation time [h]	C_{mag}	Fe content [% dry weight]
1500	2.34 ± 0.32	45.8 ± 3.1	0.31 ± 0.02	0.11
2000	2.06 ± 0.37	45.7 ± 2.9	0.38 ± 0.03	0.11
2500	2.60 ± 0.42	46.9 ± 2.7	0.31 ± 0.02	0.12
3000	2.95 ± 0.38	36.9 ± 4.1	0.33 ± 0.04	0.09
3500	2.96 ± 0.37	35.3 ± 3.2	0.32 ± 0.03	0.09

Figure S1. Photoheterotrophic growth of *R. rubrum "magneticum"* at different light intensities and cultivation temperatures. Cells were grown in 12 mL Hungate tubes in Sistrom's minimal medium supplemented with 50 µM Fe^{3+}. Cultivation was performed under microoxic conditions at 21 °C (A), 16 °C (B), or 10 °C (C). For the indicated light intensities (ranging from 1500-3500 lux), the respective generation times were calculated, as well as the final optical density (OD_{660}), the magnetic response (C_{mag}) and the iron content (given as % of dry weight) in the stationary phase. Growth curves represent the average of three biological replicates (n = 3).

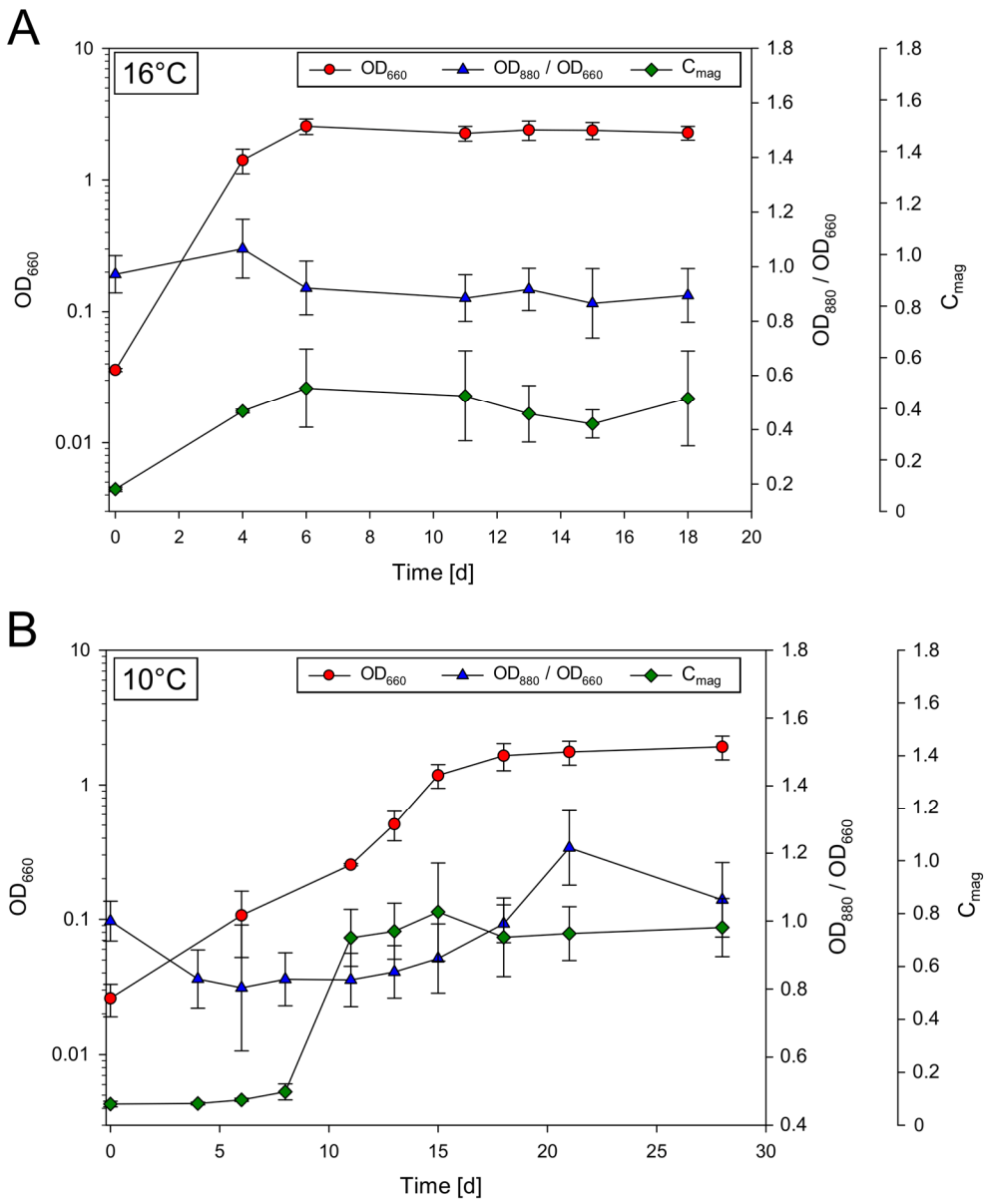

Figure S2. Growth of *R. rubrum "magneticum"* in 0.5 L culture volume. Cells were cultivated under microoxic conditions in 0.5 L Sistrom's minimal medium (supplemented with 50 µM Fe^{3+}) at 1000 lux and 16 °C (A) or 10 °C (B). For each time point of sampling, the optical density OD_{660}, OD_{880}/OD_{660} ratios and C_{mag} values were determined. Error bars represent standard deviations calculated from at least three independent measurements (biological replicates), $n \geq 3$.

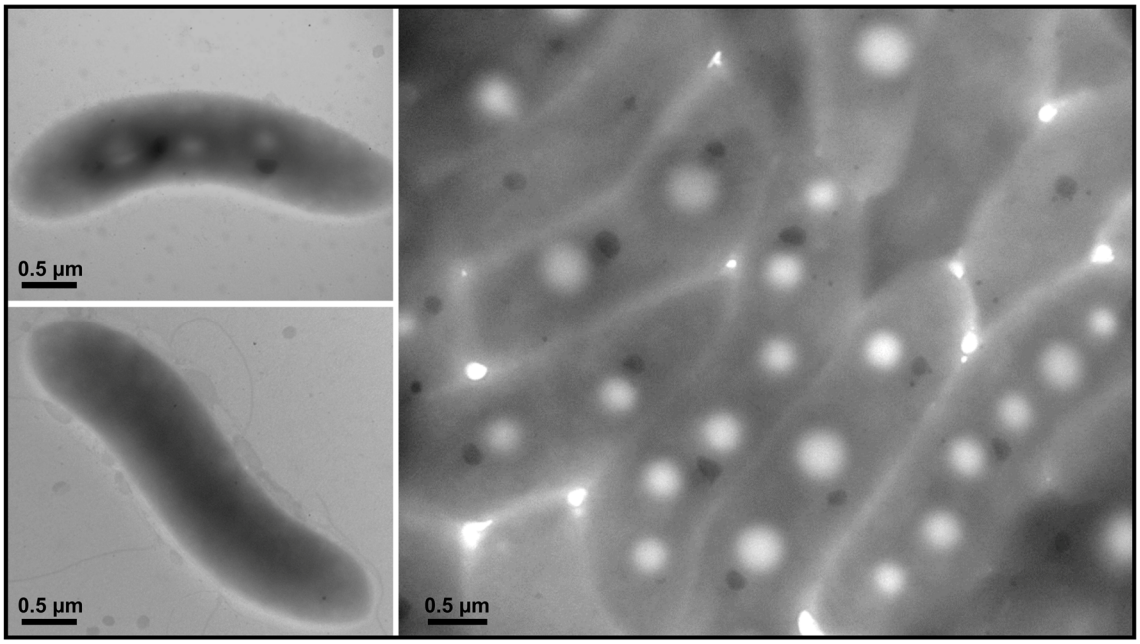

Figure S3. Transmission electron microscopy analyses of the WT strain of *R. rubrum*. The latter was grown microoxically in Sistrom's minimal medium at 10 °C, applying gradually increasing light intensities (300 - 1000 lux, depending on optical density). Under these optimized photoheterotrophic conditions, the strain could be grown to a final OD_{660} of 3.10 ± 0.23, similar to the values obtained for strain *R. rubrum "magneticum"*.

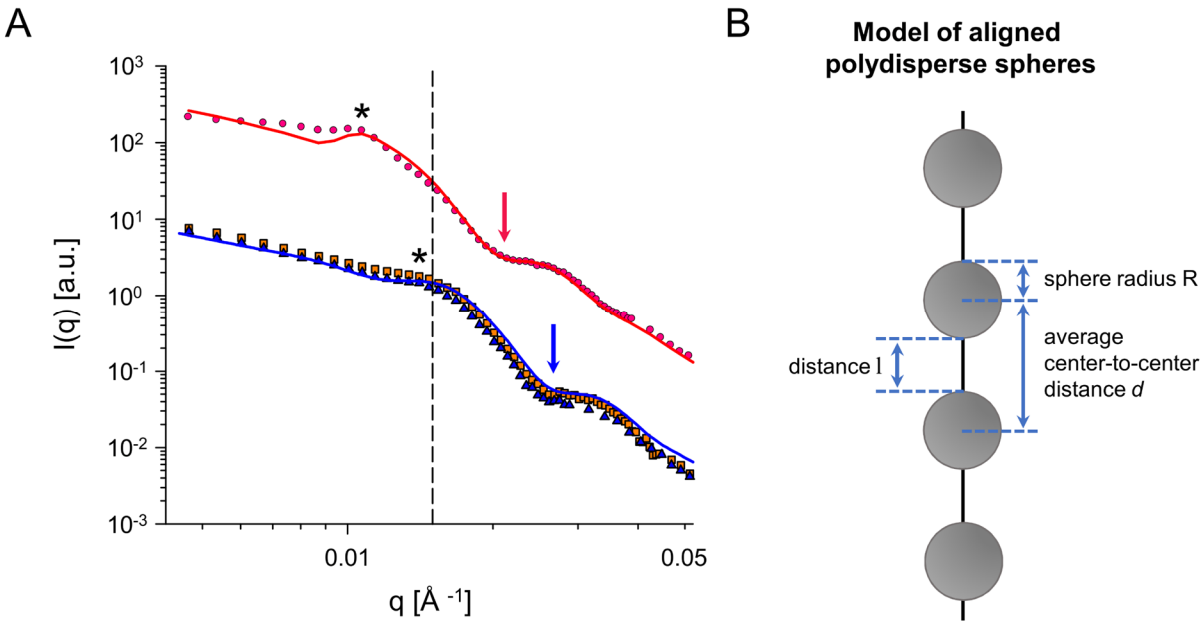

Figure S4. Characterization of magnetosomes from different organisms by SAXS. (A) Highly concentrated particle suspensions from *R. rubrum "magneticum"* (red circles, ●) or the wild type of *M. gryphiswaldense* (blue triangles, ▲) each in 10 mM Hepes / 1 mM EDTA, pH 7.2 were investigated. In addition, *M. gryphiswaldense* magnetosomes were measured in double-distilled H_2O (orange squares, ■) to exclude effects derived from the solvent. Magnetosome mean core diameters (2R, R sphere radius) with Gaussian distribution of 41 ± 7 nm (for *R. rubrum "magneticum"*) and 32 ± 5 nm (for *M. gryphiswaldense*) were obtained from the form factor minima (highlighted by arrows). The Bragg-like shoulder at scattering vectors smaller than 0.015 $Å^{-1}$ (dashed line) indicated average center-to-center distances *d* (marked by asterisks) of 63 nm (*R. rubrum "magneticum"*) and 44 nm (*M. gryphiswaldense*). A model based on (aligned) polydisperse spheres with radius R separated by a distance l was applied to fit the profiles (red line, *R. rubrum "magneticum"*; blue line, *M. gryphiswaldense*) and to interpret the data (Rosenfeldt et al. 2019; Rosenfeldt et al. 2021) yielding the following parameters: R = 20.5 ± 3.5 nm and l = 22 nm for *R. rubrum "magneticum"*, and R = 16.0 ± 2.5 nm and l = 12 nm for particles from *M. gryphiswaldense*. The model is shown schematically in (B). This analysis suggests that neighboring particles are in close proximity to each other.

Center-to-center distance $d = 2R + l$, radius of spherical core R,
distance between two spheres l (smallest distance from surface to surface of the spheres).

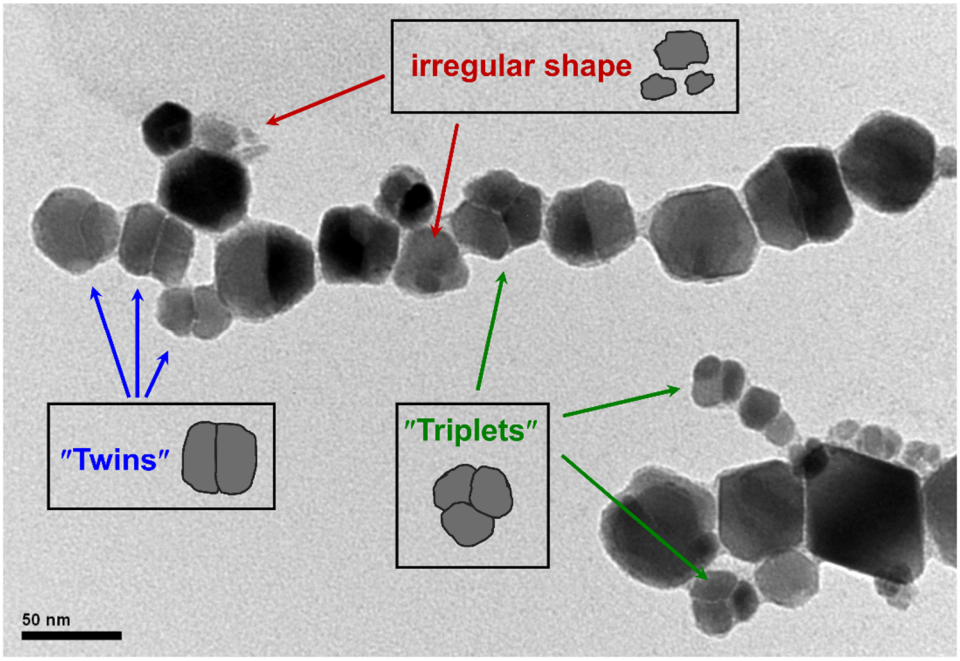

Figure S5. Transmission electron micrograph of magnetosomes from *R. rubrum "magneticum"* grown microoxically in Sistrom's minimal medium (supplemented with 50 µM Fe^{3+}) at 10 °C and gradually increasing light intensities. In suspensions of isolated magnetosomes, particles with biomineralization defects were observed to some extent, ranging from twinned crystals (19.3%, blue arrows) and triplets (3.6%, green arrows) to irregularly shaped particles (15.4%, red arrows).

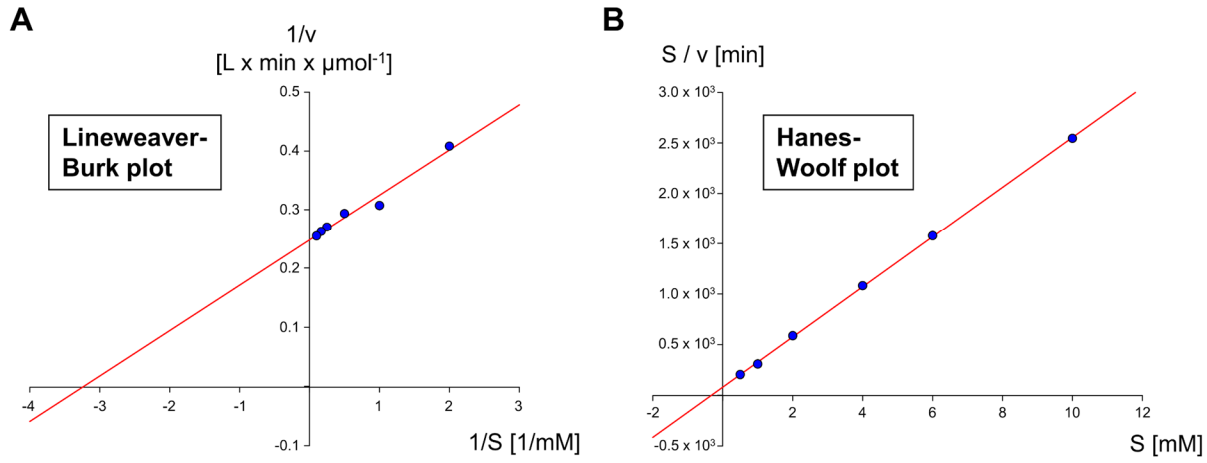

Figure S6. Lineweaver-Burk and Hanes-Woolf plot used for the determination of kinetic constants of GusA immobilized on magnetosomes from *R. rubrum_ABG6X_feoAB1_mamC-gusA*. GusA activity was determined using a modified protocol from Myronovskyi et al. (2011). GusA cleaves the artificial substrate *p*-nitrophenyl-β-D-glucuronide, yielding 3-glucuronate and *p*-nitrophenol. The time-dependent production of *p*-nitrophenol was monitored and absorption slopes were determined. The latter enabled the calculation of reaction rates (v). Lineweaver-Burk (A) and Hanes-Woolf (B) plots were subsequently used to determine the kinetic parameters K_M and v_{max} (see also Table S1). For each plot, the average of at least three independent experiments was calculated ($n \geq 3$).

Supplemental Tables

Table S1. Kinetic parameters of GusA immobilized on the surface of *R. rubrum "magneticum"* magnetosomes (strain *R. rubrum_ABG6X_feoAB1_mamC-gusA*), and specific activities given as units [U] per milligram of protein or Fe.

Kinetic parameter	Approximation			
	Michaelis-Menten	Lineweaver-Burk	Hanes-Woolf	Average
K_M [mM]	0.31	0.31	0.33	0.31
v_{max} [µmol L^{-1} min^{-1}]	3.94	4.04	4.04	4.01
Specific activities	16.54 U/mg GusA		1.22 U/mg Fe	

Table S2. Strains used in this study.

Strain	Description	Source or reference
Escherichia coli		
WM3064	*thrB1004 pro thi rpsL hsdS lacZ∆M15 RP4-1360 ∆(araBAD)567 ∆dapA1341::[erm pir]*	Metcalf, unpublished
Rhodospirillum rubrum		
R. rubrum ATCC 11170	wild type	(kindly provided by H. Grammel, Magdeburg, Germany)
R. rubrum_ABG6X_feoAB1 (*R. rubrum "magneticum"*)	Kan^R, Cm^R, Gm^R, Tc^R transposon mutant with inserted *mamAB, mamGFDC, mms6, mamXY* and *feoAB1* operon	Kolinko et al. 2014
R. rubrum_ABG6X_feoAB1_ mamC-gusA	Kan^R, Cm^R, Gm^R, Tc^R, Amp^R transposon mutant with inserted *mamAB, mamGFDC, mms6, mamXY* and *feoAB1* operons, and inserted *mamC-gusA* expression cassette from $P_{mamDC45}$	this study

Table S2. *Continued*.

Strain	Description	Source or reference
Magnetospirillum gryphiswaldense		
M. gryphiswaldense MSR-1 R3/S1	Rif^R, Sm^R, spontaneous mutant, lab strain	Schultheiss and Schüler 2003
M. gryphiswaldense MSR-1 WT::*mamC-gusA*	Rif^R, Sm^R, Kan^R, transposon mutant with inserted *mamC-gusA* from $P_{mamDC45}$	Mickoleit and Schüler 2018

Table S3. Plasmids used in this study.

Plasmid name	Description	Source or reference
pBAM1	Kan^R, Amp^R, oriR6K, *tnpA*	Martinez-Garcia et al. 2011
pSB9	pBAM1 with $P_{mamDC45}$, *mamC-gusA*, Kan^R, Amp^R	Borg, unpublished
pSB9_*amp*	pSB9 with additionally inserted ampicillin resistance cassette Amp^R upstream of $P_{mamDC45}$	this study

Table S4. Primers / oligonucleotides used in this study. Restriction sites are indicated in bold.

Primer name	Sequence (5' - 3')	Restriction site
Amp AvrII fwd	CATTTATT **CCTAGG** CCCCTATTTGTTTATTTTTCTAAAT ACATTC	AvrII
Amp EcoRI rev	GTAAAAAAT **GAATTC** GACAAGGGTCGTCCAAAAAAAAA GGCTCC	EcoRI

References Supporting Information

I. Kolinko, A. Lohße, S. Borg, O. Raschdorf, C. Jogler, Q. Tu, M. Pósfai, É. Tompa, J. M. Plitzko, A. Brachmann, G. Wanner, R. Müller, Y. Zhang, D. Schüler, *Nat. Nanotech.* **2014**, *9*, 193.

E. Martinez-Garcia, B. Calles, M. Arevalo-Rodriguez, V. de Lorenzo, *Bmc Microbiol.* 2011, *11*, 38.

F. Mickoleit, D. Schüler, *Adv. Biosyst.* **2018**, *2*, 1700109.

M. Myronovskyi, E. Welle, V. Fedorenko, A. Luzhetskyy, *Appl. Environ. Microbiol.* **2011**, *77*, 5370.

S. Rosenfeldt, F. Mickoleit, C. Jörke, J. H. Clement, S. Markert, V. Jérôme, S. Schwarzinger, R. Freitag, D. Schüler, R. Uebe, A. S. Schenk, *Acta Biomater.* **2021**, *120*, 293.

S. Rosenfeldt, C. N. Riese, F. Mickoleit, D. Schüler, A. S. Schenk, *Appl. Environ. Microbiol.* **2019**, *85*, e01513.

D. Schultheiss, D. Schüler, *Arch. Microbiol.* **2003**, *179*, 89.